OPEN

Citation: Oncogenesis (2013) **2**, e69; doi:10.1038/oncsis.2013.34

www.nature.com/oncsis

ORIGINAL ARTICLE

Centrosomal kinase Nek2 cooperates with oncogenic pathways to promote metastasis

TK Das[1], D Dana[2], SS Paroly[2], SK Perumal[3], S Singh[4], H Jhun[2], J Pendse[1], RL Cagan[1], TT Talele[4] and S Kumar[2]

Centrosomal kinase Nek2 is overexpressed in different cancers, yet how it contributes toward tumorigenesis remains poorly understood. *dNek2* overexpression in a *Drosophila melanogaster* model led to upregulation of *Drosophila* Wnt ortholog wingless (Wg), and alteration of cell migration markers—Rho1, Rac1 and E-cadherin (Ecad)—resulting in changes in cell shape and tissue morphogenesis. *dNek2* overexpression cooperated with receptor tyrosine kinase and mitogen-activated protein kinase signaling to upregulate activated Akt, Diap1, Mmp1 and Wg protein to promote local invasion, distant seeding and metastasis. In tumor cell injection assays, *dNek2* cooperated with *Ras* and *Src* signaling to promote aggressive colonization of tumors into different adult fly tissues. Inhibition of the PI3K pathway suppressed the cooperation of dNek2 with other growth pathways. Consistent with our fly studies, overexpression of human *Nek2* in A549 lung adenocarcinoma and HEK293T cells led to activation of the Akt pathway and increase in β-catenin protein levels. Our computational approach identified a class of Nek2-inhibitory compounds and a novel drug-like pharmacophore that reversed the *Nek2* overexpression phenotypes in flies and human cells. Our finding posits a novel role for Nek2 in promoting metastasis in addition to its currently defined role in promoting chromosomal instability. It provides a rationale for the selective advantage of centrosome amplification in cancer.

Oncogenesis (2013) **2,** e69; doi:10.1038/oncsis.2013.34; published online 9 September 2013

Subject Categories: Cell cycle and growth regulation

Keywords: Nek2 cancer model; metastasis; Akt; RTK; Nek2 inhibitor; *Drosophila*

INTRODUCTION

Centrosomal kinases are important regulators of cell division. They control key processes such as centrosome cycle, kinetochore–microtubule attachment, spindle checkpoint/assembly, chromosome condensation and cytokinesis. Uncontrolled activity of these kinases can lead to spindle abnormalities, centrosome fragmentation, premature centriole splitting, cytokinesis defects, multinucleation, supernumerary centrosomes and chromosome segregation errors. These cellular phenotypes, referred to as chromosomal instability (CIN), are frequently observed in transformed cells indicating that overexpression of mitotic kinases might drive tumor progression *in vivo* by promoting CIN.[1,2] Yet a clear notion of the mechanism by which these kinases contribute to tumorigenesis remains elusive.

Never-In-Mitosis-A-related kinase 2 (Nek2) is a serine/threonine kinase that has a critical role in mitosis during the cell division process.[3] Uncontrolled Nek2 activity can lead to CIN as well as abnormal chromosome content—often 2–3 times the content of a normal diploid cell.[4] Expression of Nek2 is elevated (three to fivefold) in different forms of cancer cell lines, including invasive cancer cells.[5] In xenograft studies, uptake of Nek2 siRNA into the tumor significantly reduced tumor size, suggesting Nek2 inhibition can counter tumor progression *in vivo*.[6] These findings suggest that Nek2 regulates tumor progression *in vivo* and that Nek2 inhibition could be useful for developing anti-cancer therapeutics. But like the other centrosomal kinases, the role of Nek2 in tumor progression remains unclear.

Modeling cancer in cell lines has not fully captured the complex cellular behavior of this disease.[7] Whole-animal mouse cancer models have proven useful in understanding programs of tumor progression, but have been too costly and time-consuming to develop for an expansive study of large numbers of cancer-related genes.[8] Recently the fruit fly, *Drosophila melanogaster*, has been used to identify novel cancer risk factors indicating the enormous translational potential of flies for modeling cancer.[9–12]

We have developed and characterized the first whole-animal Nek2 overexpression model using *Drosophila melanogaster*. Overexpression of the fly Nek2 ortholog (dNek2) in developing fly tissues led to increased centrosome number. It also enhanced cell migratory behavior leading to distant seeding of cells. Molecular analysis revealed that *Nek2* overexpression led to upregulation of secreted Wg protein, deregulation of Ecad, Rho1, Rac1 and activation of Akt, proteins that are intricately connected to the process of cell survival and migration. *Nek2* cooperated with receptor tyrosine kinase (RTK), *Ret*, to enhance local invasion, distant seeding of cells as well as to increase the levels of the activated Akt protein. *Nek2* also cooperated with intracellular signaling molecules, activated *Ras* and *Src*, to increase Mmp1, Diap1 and Wg protein levels and drive metastasis. Using a novel tumor cell injection assay in flies, we established that *Nek2*-overexpressing cells could cooperate with other oncogenic pathways to aggressively colonize various tissues in the adult fly. Genetic or pharmacological inhibition of the PI3K pathway

[1]Department of Developmental and Regenerative Biology, Mount Sinai School of Medicine, New York, NY, USA; [2]Department of Chemistry and Biochemistry, Queens College and the Graduate Center of the City University of New York, Queens, NY, USA; [3]Department of Chemistry, The Pennsylvania State University, University Park, PA, USA and [4]Department of Pharmaceutical Sciences, College of Pharmacy and Health Sciences, St. John's University, Queens, NY, USA. Correspondence: Professor S Kumar, Department of Chemistry and Biochemistry, Queens College and the Graduate Center of The City University of New York, 65-30 Kissena Blvd, Queens, NY 11367-1597, USA.
E-mail: Sanjai.Kumar@qc.cuny.edu
Received 25 June 2013; revised 23 July 2013; accepted 29 July 2013

suppressed the cooperation phenotypes with Ret as well as Ras and Src signaling, indicating that PI3K is a key effector pathway downstream of Nek2 driving tumorigenesis. Overexpression of human Nek2 in human cell lines also deregulated similar signaling pathways leading to stabilization of β-catenin protein levels and reduced β-catenin at the membranes, phenotypes consistent with a pro-invasive state.

Currently there is considerable effort in trying to identify potent and non-toxic small molecule inhibitors that inhibit Nek2 function. By proceeding from virtual screening, to *in vitro* testing, to using our fly model, we rapidly identified drug-like compounds most optimal for Nek2 inhibition *in vivo*.

Our studies have uncovered a novel role for Nek2 in promoting tumorigenesis by regulating an axis of metastasis and cell survival. We have also identified a new set of Nek2 inhibitors, and delineated a novel inhibitory pharmacophore for Nek2 kinase. Our studies continue to highlight the advantages of combining whole-animal genetic studies with rational drug discovery to yield compounds with optimal therapeutic index.[13]

RESULTS

Drosophila Nek2 overexpression model

We first established if studying the *Drosophila* Nek2 ortholog would be likely to recapitulate the kinase function of human Nek2. Primary sequence alignment analysis (BLAST) of human and *Drosophila* Nek2 kinase domains revealed that they shared a high degree of amino-acid sequence conservation (Figure 1a—70% sequence similarity and 50% sequence identity of amino-acid residues in the N-terminal kinase domain). As the *Drosophila* Nek2 crystal structure is unavailable, a homology model was generated using human Nek2 (PDB ID: 2JAV) as a template.[14] A striking similarity between the fly and human protein structures is evident at both secondary and tertiary structure level (Figure 1b), including a high degree of conservation of the key active site residues (Figure 1c). The fly ortholog possesses important motifs present in most kinase family members—hinge loop, HRD and DFG motifs.[14] Key residues required for optimal activity of human Nek2 were also retained in the fly ortholog: amino-acid residues of the activation segment and the autophosphorylation sites. In addition, residues in human Nek2 that can be changed to increase or decrease kinase activity *in vitro* were also conserved in the *Drosophila* ortholog.[15] Thus, a high conservation of these key features suggested that fly Nek2 likely retains the key physiological functions of its human counterpart.

We therefore generated a *Drosophila* Nek2 overexpression model that allowed us to target inducible expression of dNek2 to specific tissues using the GAL4-UAS system.[16] We generated a C-terminal fusion with green fluorescent protein (GFP) (*UASdNek2-GFP*) to allow us to monitor the subcellular localization of ectopic Nek2.

dNek2 overexpression leads to increased levels of Wg and activated Akt

To establish if overexpression of *Drosophila Nek2* could recapitulate key features of human Nek2 function, we monitored the status of centrosomes. Overexpression of *dNek2* in the peripodial cells of the developing wing epithelium (*ptc > dNek2-GFP*; Figure 2a, centrosomal marker γ-tubulin) led to an increase in the number of centrosomes. While some dNek2-GFP-expressing cells had the usual 1–2 centrosomes per cell, others showed an increase to 3–5 per cell (Figure 2a, cells outlined in red). As predicted, Nek2-GFP signal was enriched over the centrosomes and in some other subcellular regions. Overexpression of vertebrate *hNek2* in cultured cells led to a similar increase in centrosome numbers, indicating that our model phenocopied features of human Nek2 overactivity.[3]

To uncover potentially novel roles for this kinase, we next overexpressed *dNek2* in other developing tissues. Overexpression of *dNek2* in the thorax led to incomplete closure of the notum, abnormal patterning of the bristles and a severe defect in the scutellum (*pnr > Nek2GFP*; Figure 2c, abnormal patterning of notum hairs—asterisk and malformed scutellum—arrow). The notum and scutellum arise from the fusion of tissues from the proximo-dorsal portion of the two wing discs. Altered activity of regulators of cytoskeletal dynamics and cell migration in the notum/scutellum can lead to similar tissue defects, e.g., activation of the Jun N-terminal kinase (Jnk) pathway.[17] *dNek2* overexpression in the developing eye led to extensive mispatterning and positioning of ommatidia leading to a 'rough eye' phenotype in the adult (Figure 2e). *dNek2* overexpression along the anterior-posterior (A/P) boundary of the wing disc resulted in severe disruption of adult wing vein pattern (*ptc > Nek2-GFP*; Figures 2f and g). As Nek2-GFP overexpression does not result in caspase activation in larval discs (data not shown), this altered adult wing phenotype is not likely due to increased cell death. Morphogens such as wingless (Wg) and decapentaplegic (Dpp) regulate the patterning of the developing wing disc along its axes.[18] Wg is expressed strongly in the dorso-ventral boundary of the wing disc and at the edge of the pouch region, but only very low levels are detectable in other areas of the wing disc. *dNek2* overexpression led to a significant increase in Wg protein levels across the entire wing disc, which accumulated at distance from the dNek2 expression domain (Figures 2h and i, asterisks, i′), indicating dNek2 promoted secretion of Wg protein. *dNek2* overexpression also led to a significant alteration in size and shape of the entire tissue indicating an effect on signaling pathways that drive tissue morphogenesis (Figures 2j and k). In addition, levels of adherens junction component Ecad, a protein that is frequently down-regulated before cell invasion,[19] was also reduced in Nek2-overexpressing cells (Figures 2l and l′). To understand which signaling pathways Nek2 kinase was upregulating, we next performed western analysis on wing discs.

Immunoblot analysis of wing disc tissues overexpressing *dNek2* showed consistently higher levels of pAkt (*765 > Nek2GFP*; Figure 2m), which is another bonafide regulator of growth, migration and survival[20] and is consistent with the observed increased in thickness of the wing disc (Figure 2k). Overexpression of *dNek2* also altered relative levels of Rho-GTPase family proteins Rho1 and Rac1. Through their antagonistic activities, these proteins are central to driving actin–tubulin dynamics and cell migratory behavior.[21] We observed a decrease in Rho1 levels and an increase in Rac1 levels, suggesting a disruption in the balance of cytoskeletal dynamics of normal epithelium. Finally, overexpression of *dNek2* also led to decrease in adherens junction component Ecad, as we had observed in our immunofluorescence experiments in Figure 2l.

These experiments established three novel findings: Nek2 overexpression leads to secretion of increased levels of Wg, activation of Akt, and alteration in the levels of Rho1, Rac1 and Ecad proteins. All of these can have a significant impact on tumor progression.

dNek2 cooperates with RTK signaling to regulate invasion and differentiation

We next investigated if Nek2 overexpression can cooperate with other signals by coexpressing *dNek2* with an oncogenic isoform of the RTK Ret, $dRet^{MEN2}$. This fly model recapitulates essential features of Ret^{MEN2} oncogenic signaling, and was used to identify a novel program of invasion/metastasis in humans.[10,22]

Coexpression of *dNek2* and $dRet^{MEN2B}$ in stripes of cells along the anterior-posterior (A-P) wing-disc compartment boundary led to migration of a large number of GFP + cells into the adjacent compartment (non-GFP) with normal cells (*ptc > Nek2-GFP,*

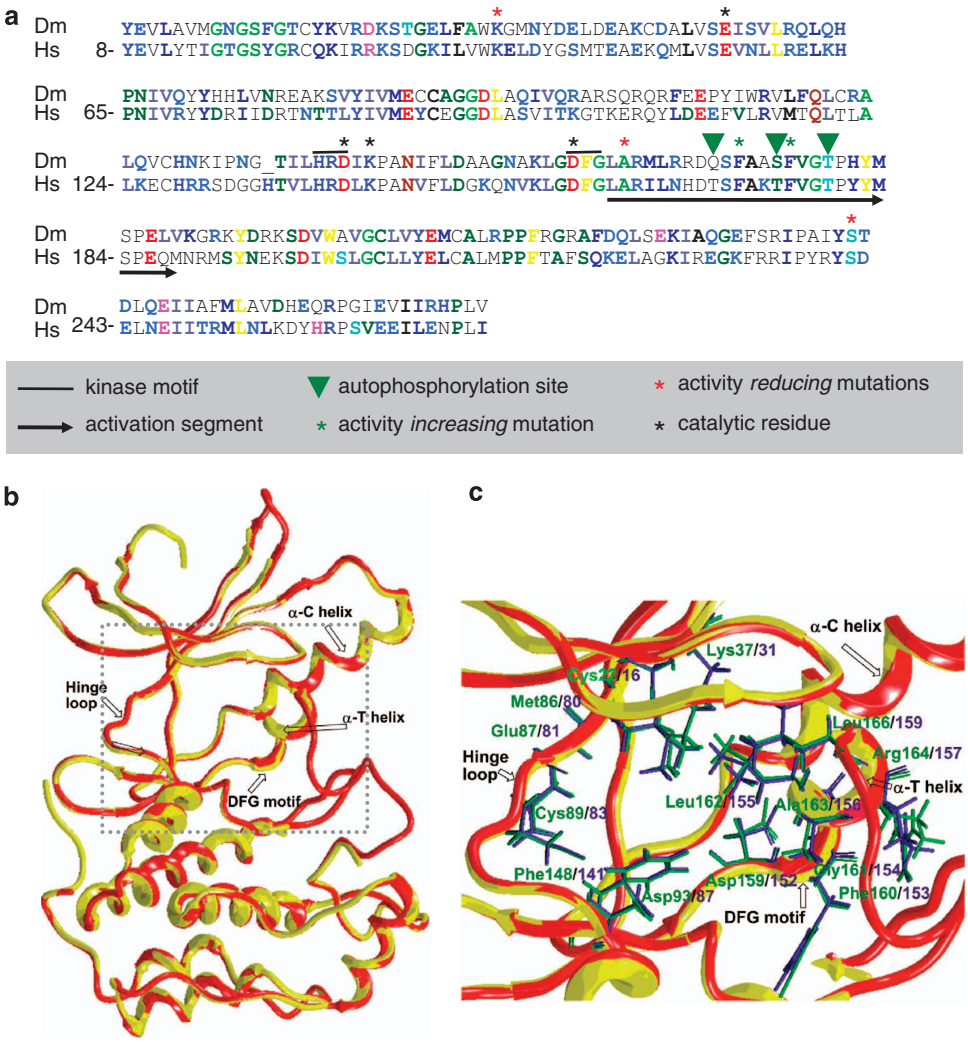

Figure 1. (**a**) Primary sequence alignments shows that N-terminal region of hNek2 and dNek2 share 70% amino-acid sequence similarity and 50% identity. Key functional residues of hNek2 are indicated in the legend below. A significant number of these key residues are conserved in dNek2. (**b**) Ribbon diagram of the superimposed view of the homology model-generated *Drosophila* (red) and human (yellow, (PDB ID: 2JAV)) Nek2 kinase structures. A striking similarity is evident between the two at the secondary and tertiary structure levels. (**c**) A close view of key active site residues of human (green) and *Drosophila* (violet) Nek2 kinase, depicted as sticks.

Ret^{MEN2B}; Figures 3a, c and e). Expression of oncogenic Ret alone enhanced proliferation but had little effect on migration, and very few cells migrated away from A-P boundary (*ptc* > Ret^{MEN2B}; Figures 3b–d). Combined *dNek2* and $dRet^{MEN2B}$ expression also resulted in extensive rearrangement of the cytoskeletal tubulin network (Figure 3e; α-tubulin), whereas expression of oncogenic Ret alone had minimal effect on the organization of this network (Figure 3d). Together, these findings indicated that dNek2 and $dRet^{MEN2B}$ signals cooperated to provoke dramatic alteration of cytoskeletal organization and promote cell migration.

Next we tested if dNek2 and oncogenic Ret signaling also synergized in very few, clonally propagating, groups of cells using the *eyeless-FLPase-MARCM* system.[23] In this method, clonal cells expressing transgenes also express *GFP*. Control flies with clones of only GFP-expressing cells had normal adult eyes with visible clones of GFP + cells interspersed with non-GFP cells (Figure 3f). Expression of Ret^{MEN2B} resulted in compensatory proliferation and apoptosis during development leading to very rough eyes with overgrown, but fully differentiated tissue (Figure 3g, red pigmentation). Coexpression of *dNek2* and Ret^{MEN2B} led to a significantly larger population of GFP + cells in the larval eye discs (Figures 3i and j), indicating a growth advantage with this combination. Large groups of GFP + cells were also seen in neighboring tissues such as the proboscis (Figures 3h and h′, arrowheads). Interestingly, we noticed the emergence of large GFP + outgrowths that did not have pigmentation (Figures 3h and h′, arrowheads), indicating these cells were not differentiated. Loss of differentiation or maintenance of cells in a naïve, undifferentiated state is another feature of cancer cells.[19] We therefore looked at the expression of differentiation markers at earlier developmental stages of the larvae. While expression of Ret^{MEN2B} maintained strong expression of differentiation marker protein Elav (elav) (Figure 3i), coexpression of *dNek2* and Ret^{MEN2B} led to strong reduction of elav both inside and outside the GFP^+ clones, suggesting differentiation of the cells was being compromised (Figures 3j and j′; arrowheads). Reduction of elav expression non-autonomously outside the GFP^+ clones suggested that Nek2 could affect tumor progression autonomously (yellow arrowhead) as well as non-autonomously (white arrowhead), perhaps via secreted ligands such as Wg.

dNek2 cooperates with oncogenic Ras and Src signaling to promote survival and metastasis

We next tested if Nek2 could cooperate with other intracellular oncogenic signaling pathways. Activated Ras and activated Src are

common features in many cancers and the Cagan laboratory had previously established a fly model where both these pathways are activated.[24] Simultaneous activation of Ras and Src pathways using the *eyeless-FLPase-MARCM* system led to limited tissue overgrowth in larval eye discs (Figure 4b; *Csk −/−; Ras^{V12}*). Coexpression of *dNek2* along with activated Ras and Src led to significant overgrowth of GFP^{+} tissue (Figure 4c; *dNek2*; *Csk −/−; Ras^{V12}*, arrows) as well as appearance of secondary tumors in the body of the larvae (Figure 4c, asterisk). *dNek2; Csk −/−; Ras^{V12}* cells showed significantly higher levels of inhibitor of apoptosis (Diap1), matrix metalloprotease (Mmp1), Wg, as well as cell cycle regulator protein CycE, compared with *Csk −/−; Ras^{V12}* cells (Figures 4d–k). Cooperative upregulation of these proteins indicates that *dNek2* enhanced the tumorigenic potential of *Csk −/−; Ras^{V12}* cells. Upregulation of Wg protein could also promote growth of neighboring tumor cells non-autonomously, allowing *dNek2*-overexpressing cells to en-masse promote tumorigenesis in a large group of cells.

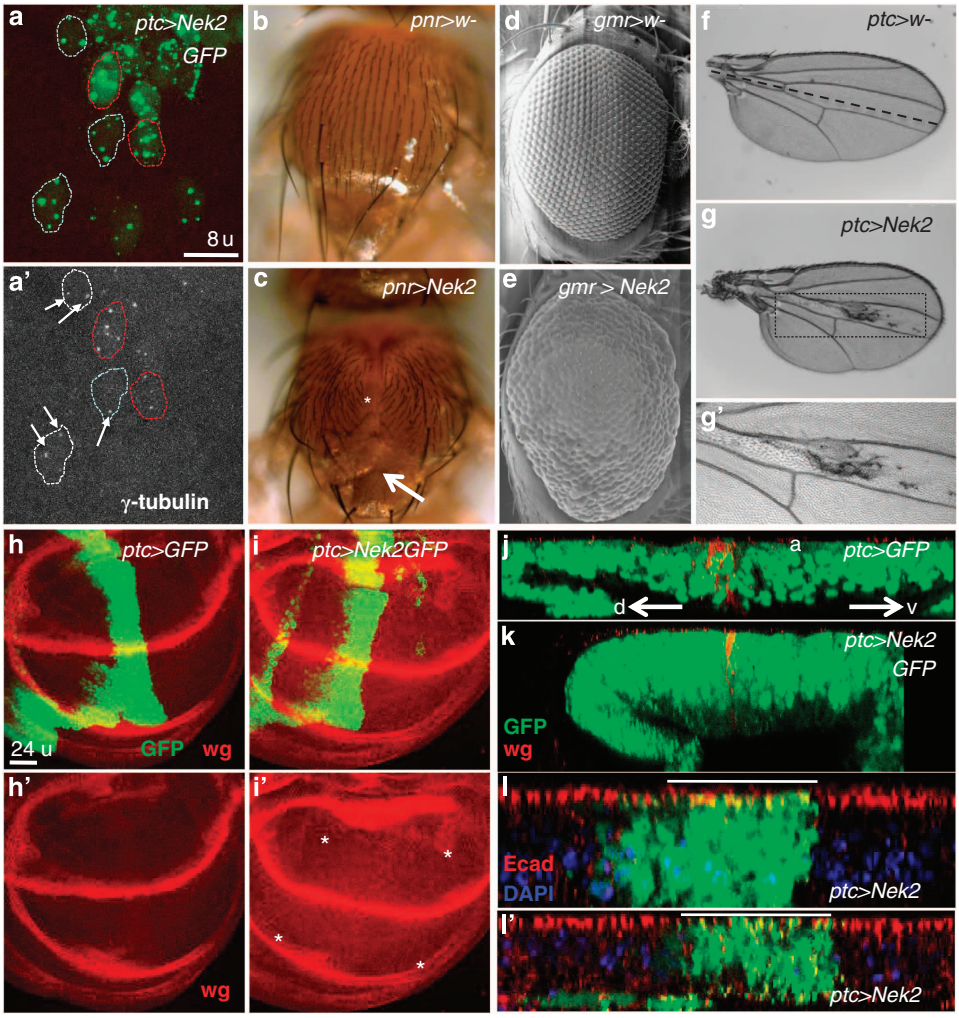

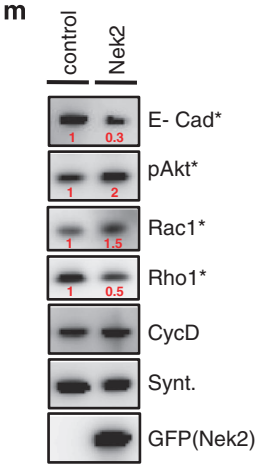

To address whether *dNek2; Csk −/−; Ras^{V12}* cells could colonize differentiated tissues in the adult, we developed a new tumor cell injection assay. Dissociated *dNek2; Csk −/−; Ras^{V12}* cells were injected into the dorsal notum region of wild-type (WT) adult flies, and within 10 days of injection GFP^{+} cells could be seen in various parts of the adult body (Figure 4l). Injection of *dNek2* cells (Figure 4l) or *Csk −/−; Ras^{V12}* cells (data not shown) did not result in detectable tumor populations in other body parts similar to our findings in the larvae (Figures 4a–c). This assay is akin to tail-vein injection protocol in mice and allows for a large number of injections to be performed and tumors to be analyzed, and is a significant improvement over current tumor transplantation assays in flies.[25]

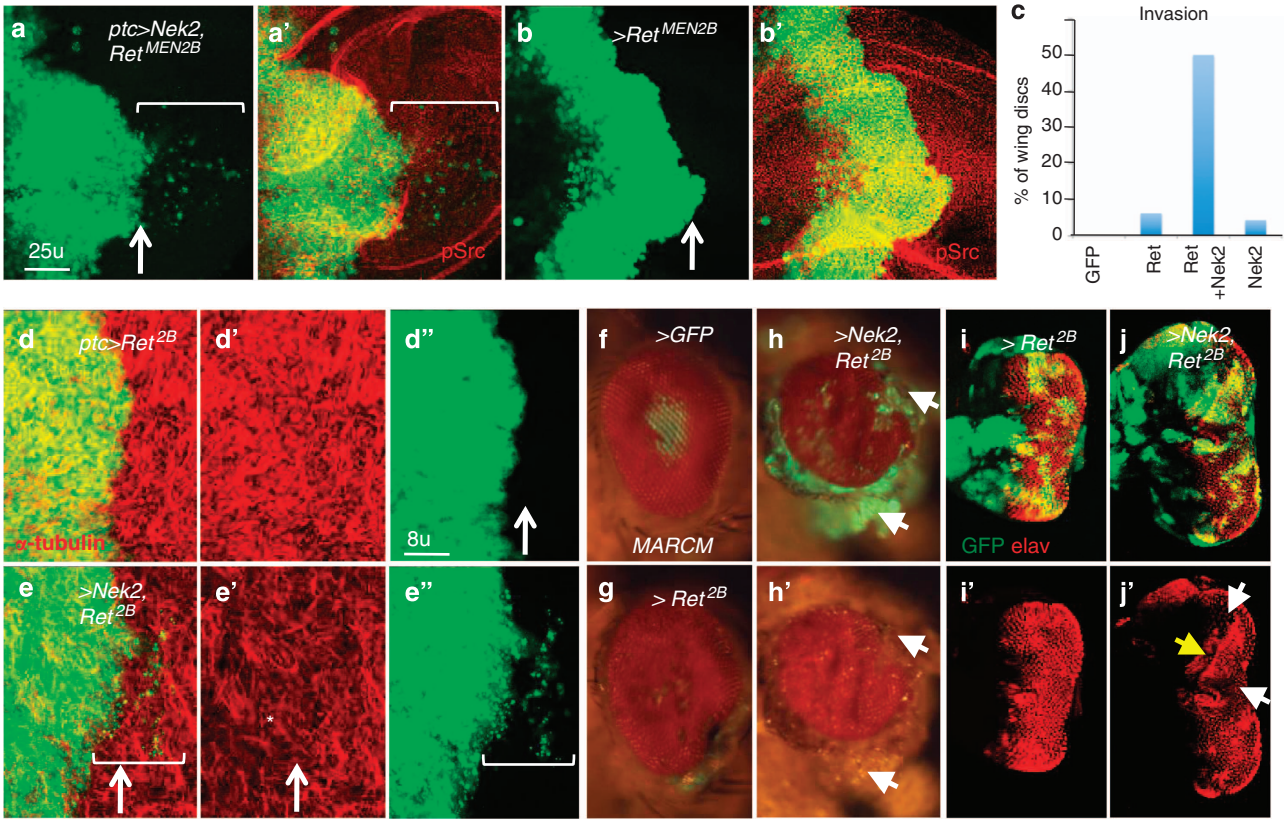

Figure 3. (**a**, **b**) Coexpression of dNek2-GFP and Ret^{MEN2B}, *ptc > dNek2-GFP, Ret^{MEN2B}*, in the developing wing discs led to large number of GFP + cells migrating away (bracket) from the anterior-posterior boundary (arrow) (**a**, **a**′). Expression of Ret^{MEN2B} alone showed almost no cell migration (**b**, **b**′). These effects were quantitated and represented in **c** showing proportion of wing discs with migration phenotypes. Number of discs analyzed for each experiment, GFP = 45, Ret^{MEN2B} = 32, dNek2-GFP(+)Ret^{MEN2B} = 36, dNek2-GFP = 23. (**d**, **e**) Coexpression of dNek2-GFP and Ret^{MEN2B} in the wing discs like in **a** and **b** led to severe alteration of polymerized tubulin network (**e**, **e**′) detected with α-tubulin antibody. Extensive migration of cells is shown in **e**′′. Little effects is seen on the polymerized tubulin network in wing discs expressing only Ret^{MEN2B} (**d**, **d**′) and consequently very little cell migration (**d**′′). (**f**–**h**) *eye-FLP-MARCM* experiments: (**f**) Control flies expressing only *UAS-GFP* showed a mixture on GFP + and non-GFP cells as would be expected from clonal propagation. (**g**) Expression of *Ret^{MEN2B}* led to very rough eyes, which retained pigmentation. (**h**, **h**′) Coexpression of *dNek2-GFP* and *Ret^{MEN2B}* led to enhancement of the rough eyes, emergence of undifferentiated GFP + tissues without pigmentation (**h** and **h**′, arrowheads), and a large increase of GFP + cells in tissues adjacent to the eye (**h**, arrowheads). (**i**, **j**) *eye-FLP-MARCM* experiment (as in **f**–**h**) eye discs stained with cell differentiation marker elav at the third instar stage, stained. Coexpression of *dNek2-GFP* and *Ret^{MEN2B}* (**j**, **j**′), compared to expression of *Ret^{MEN2B}* alone (**i**, **i**′), led to severe disruption of differentiation of cells both autonomously (GFP^{+}, yellow arrowhead) as well as non-autonomously (white arrowhead).

Figure 2. (**a**) dNek2 overexpression leads to centrosome amplification. Overexpression of dNek2, *ptc > dNek2-GFP*, in peripodial cells of the wing disc resulted in centrosome amplification. In **a**′, γ-tubulin, a centrosomal marker, shows 1–2 centrosomes (arrows) in some dNek2-GFP-expressing cells (white outline) and 3–5 centrosomes in other dNek2-expressing cells (red outline). In **a**, GFP signal distribution of dNek2-GFP, some of which localizes strongly over centrosomes. (**b**, **c**) dNek overexpression in the thorax leads to notum and scutellum defects, *pnr > dNek2-GFP* (**c**), compared with control (**b**). (**d**, **e**) dNek2 overexpression in the eye, *gmr > dNek2-GFP*, led to patterning defects in the eye (**e**) leading to disruption of the normal ordered hexagonal array of ommatidia (**d**). (**f**, **g**) dNek overexpression in the anterior-posterior boundary of the developing wing disc, *ptc > dNek2-GFP*, led to abnormal veination pattern of the adult wing (**g**) compared with control (**f**). Magnified view of boxed in (**g**) is showed in (**g**′). (**h**, **i**) Wg protein levels are increased in third instar larval wing discs overexpressing Nek2, *ptc > dNek2-GFP* (**i**) compared with control (**h**). Asterisks in **i**′ indicates higher levels of secreted Wg signal away from the *patched* (GFP^{+} cells) boundary compared to control **h**′. Images shown are confocal z-stack overlays encompassing the entire thickness of the disc. (**j**, **k**) A cross-sectional view (*y*–*z* plane) across of z-stack overlay in **h** and **i** shows the enormous difference in tissue size and shape between normal (**j**) and Nek2-overexpressing cells (**k**). a, apical; d, dorsal; v, ventral. (**l**, **l**′) A cross-sectional view (*x*–*z* plane) of wing discs where Nek2-overexpressing cells (green) show reduced levels of Ecad protein at junctions. White line shows region of reduced Ecad levels (two examples shown). Some Ecad is seen internally away from the apical region, either due to basal migration or due to some multilayering of cells. (**m**) Western analysis of larval wing disc tissues with dNek2-GFP overexpression throughout the entire disc, *765 > dNek2-GFP*. Asterisks indicate markers that were

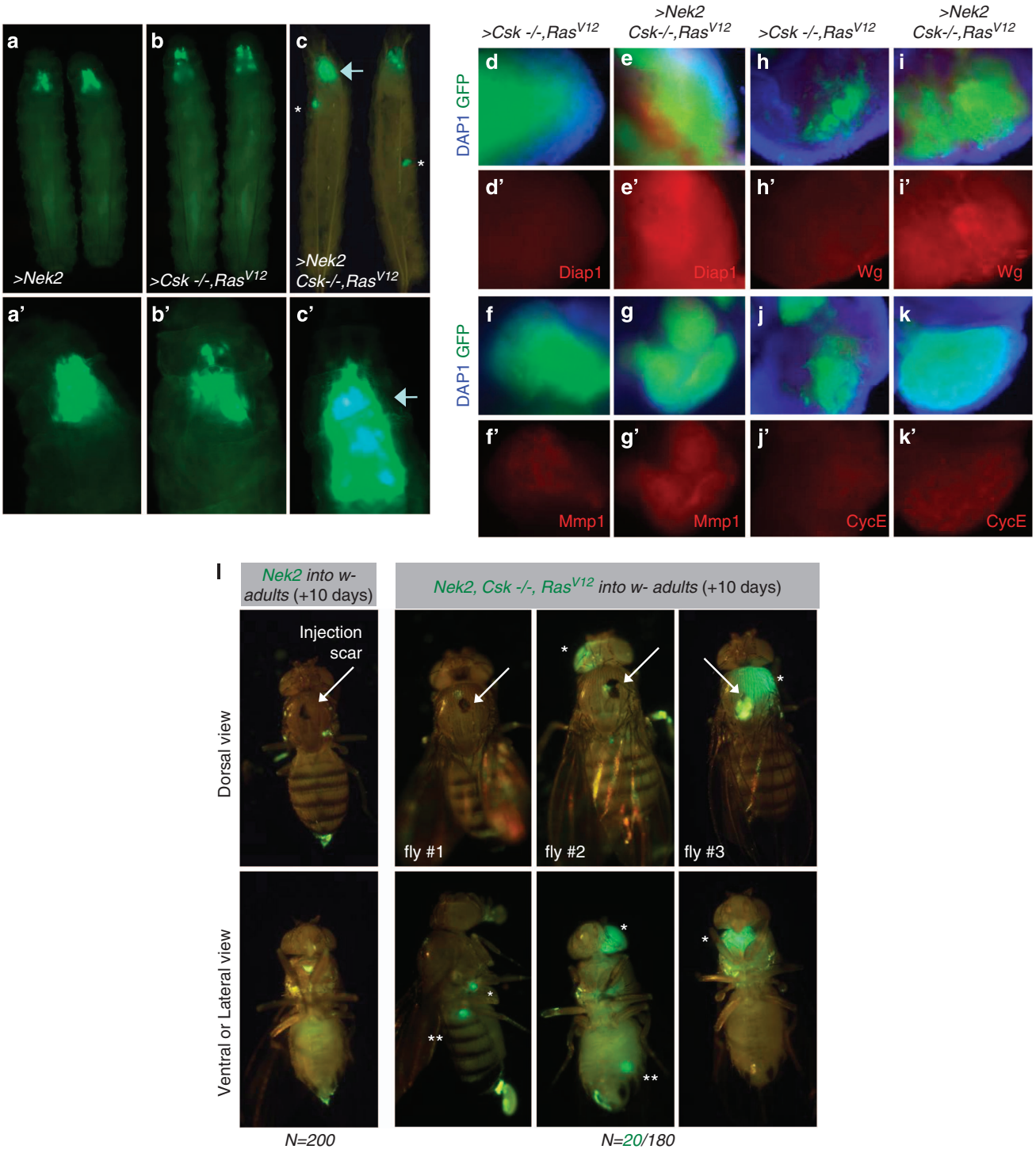

Figure 4. (**a**–**c**) *eye-FLP-MARCM* experiments showing GFP$^+$ tissues (close-up view in bottom panels **a**′, **b**′, **c**′) with the genotypes d*Nek2GFP* (**a**, **a**′), *Csk −/−; Ras^{V12}*(**b**, **b**′) and d*Nek2GFP*; *Csk −/−; Ras^{V12}* (**c**, **c**′). *dNek2GFP*; *Csk −/−; Ras^{V12}* larvae show a significant increase in primary tumor mass (arrows in **c** and **c**′) as well as appearance of secondary tumors (asterisks in **c**) at a distance from the primary tumors. (**d**–**k**) *eye-FLP-MARCM* experiments showing that *dNek2GFP*; *Csk −/−; Ras^{V12}* tissues upregulate Diap1 (**e**, **e**′), Mmp1 (**g**, **g**′), Wg (**i**, **i**′) and CycE (**k**, **k**′), in comparison with *Csk −/−; Ras^{V12}* tissues (**d**, **d**′, **f**, **f**′, **h**, **h**′, **j**, **j**′). Epifluorescence′ images were taken at equivalent settings for each channel. (**l**) Tumor cell injection experiments. GFP$^+$ *eye-FLP-MARCM* tissues obtained from third instar larvae were dissociated and injected into the dorsal notum of w- adult flies. Injection of *dNek2GFP* cells ($n = 200$) or *Csk −/−; Ras^{V12}* cells (data not shown) did not lead to GFP$^+$ cells seeding into the host fly. But injection of *dNek2GFP*; *Csk −/−; Ras^{V12}* cells led to appearance of distinct GFP$^+$ foci within 10 days of injection (20 out of 180 injected flies showed seeding injected tumor cells). Site of injection is visible as a dark scar (arrow) and three examples are shown with tumor foci in parts of the body away from the injection site (asterisks).

Taken together, these findings suggested that dNek2 could cooperate with oncogenic signaling pathways to promote survival, invasion, and metastasis and help tumor cells colonize a wide range of tissue types.

Cooperativity between dNek2 and oncogenic pathways depends on PI3K-Akt signaling

To understand the molecular mechanism underlying the cooperativity between Nek2 and oncogenic signaling pathways, we monitored intracellular signaling markers using western analysis. We found that combined *dNek2* and Ret^{MEN2B} expression throughout the wing disc resulted in higher levels of pJnk and pErk activity, compared with WT tissue (*765 > dNek2*, Ret^{MEN2B}; Figure 5a). These markers are involved in promoting cell migration, and presence of higher levels of these proteins compared with WT tissue is consistent with our migration phenotypes. Interestingly, the levels of activated Akt (pAkt) were much higher with combined *dNek2* and Ret^{MEN2B} compared with *dNek2* or Ret^{MEN2B} expression alone, suggesting that pAkt was being activated in a combinatorial manner (Figure 5a, asterisk). Similar results were observed for cooperative interaction between *dNek2* and *Ras* plus *Src* signaling. Levels of pAkt were upregulated in a combinatorial manner and levels of pJnk, Rho1 and Rac1 were also at high levels in the triple genetic combination (Figure 5b). One outcome of increased Akt activity is the inhibition of GSK3β activity that leads to the stabilization of β-catenin ortholog armadillo (Arm).[26] Indeed *dNek2* as well as *dNek2*; *Csk −/−*; Ras^{V12} tissues showed significant upregulation

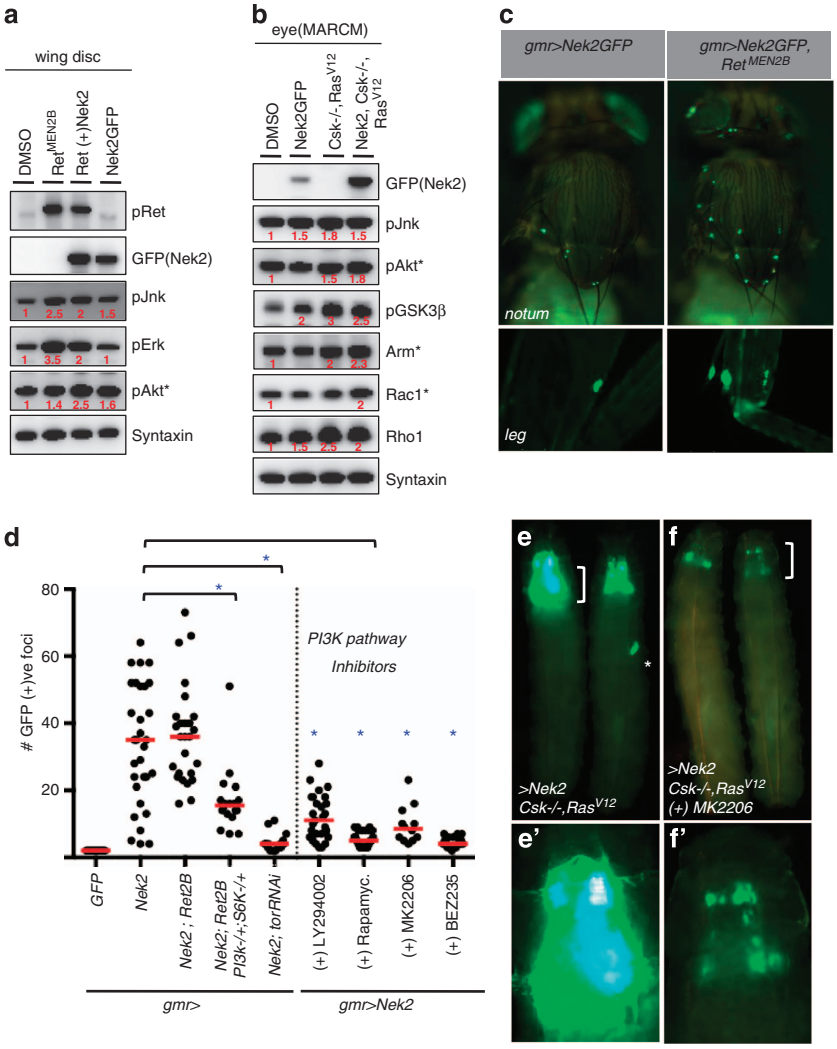

Figure 5. (**a**) Western blot analysis of wing disc tissues following coexpression of dNek2-GFP and Ret^{MEN2B}, *765d > Nek2-GFP*, Ret^{MEN2B}. pJnk and pErk are maintained at high levels in tissues coexpressing Nek2-GFP and Ret^{MEN2B}. pAkt is the only marker (asterisks) whose levels are increased above pAkt levels from expression of dNek2 or Ret^{MEN2B} alone. (**b**) Western blot analysis of eye-disc tissues using the MARCM method following coexpression of dNek2-GFP and dNek2-GFP, $RasV^{12}$, Csk −/−. pAkt level is increased combinatorially (asterisk). pGSK3β and armadillo levels are also high, with armadillo levels marginally higher in the triple combination (asterisk). Relative levels of proteins are indicated in red below each blot. Asterisk indicates markers whose levels are upregulated combinatorially. (**c**) Expression of dNek2-GFP in the developing eye, *gmr > dNek2-GFP*, led to appearance of GFP^+ foci in other tissues. Shown here are examples of foci in the thorax and legs (left panels). Coexpression of Nek2-GFP and Ret^{MEN2B} led to larger foci appearing in similar regions of fly, suggesting a more stable seeding process (right panels) without overall increase in the number of distantly seeded tumors (see quantitation in **d**). (**d**) Distant seeding in *gmr > dNek2-GFP* flies can be suppressed by genetic or pharmacological inhibition of components of the PI3K pathway. Scatter plot, where each dot represents total number of GFP^+ foci in one fly. Red line represents median. *dNek2* = 35, *dNek2;Ret2B* = 36, *dNek2;Ret2B;PI3K −/+;S6K −/+* = 15.5, *dNek2* + LY294002 (100 μM) = 11, *dNek2* + Rapamycin (1 μM) = 5, *dNek2* + MK2206 (20 μM) = 8.5, *dNek2* + BEZ235 (5 μM) = 4. Indicated doses represent final concentration of drug in food that developing larvae ate. Brackets and blue asterisks indicate *P*-values <0.05 as determined by two-tailed students *t*-test. (**e**, **f**) *dNek2GFP*; *Csk −/−*; Ras^{V12} *eye-FLP-MARCM* tissues from larvae that were fed with Akt inhibitor MK2206 (20 μM) led to inhibition of growth of primary tumors (**f**, **f′**) [bracketed area enlarged in **f′**] compared with untreated tissues (**e**, **e′**).

of pGSK3β (inhibitory phosphorylation), and in the latter case significant upregulation of *Drosophila* Arm (Figure 5b, asterisk). Thus, cooperative activation of Akt by dNek2 leads to increased levels of β-catenin ortholog armadillo, which is another potent oncogenic signal.[19]

The PI3K-Akt pathway is a well-known regulator of growth, survival and invasion/metastasis in vertebrate cancer as well as in *Drosophila*.[20,27] Therefore, enhanced activation of pAkt by dNek2 could be the primary cause for the increased survival, migration and metastasis phenotypes. To test the requirement of the PI3K-Akt pathway in promoting Nek2-dependent cooperation, we developed another quantitative assay of cell migration. Targeting *dNek2* expression to the eye, which has high levels of endogenous RTK activity, (but not GFP alone; Figures 5c and d) resulted in a large number of GFP+ spots appearing in other parts of the adult flies, including the notum, wing and legs (*gmr>dNek2-GFP*; Figures 5c and d), a phenomenon we call 'distant seeding'. Nek2-dependent distant seeding of cells was strongly suppressed by knockdown of *Drosophila tor* (*gmr>dNek2-GFP, torRNAi*), indicating the requirement of the Akt pathway for this process. Coexpression of *dNek2* and Ret^{MEN2B} resulted in larger groups of cells visible in distant body parts (*gmr>dNek2-GFP,* Ret^{MEN2B}; Figure 5c), showing again that cooperation between dNek2 and Ret^{MEN2B} promoted survival of cells in the process of 'distant seeding'. In this context, reducing PI3K pathway activity by removing a genetic copy of PI3K as well as S6K significantly reduced the distant seeding phenotype (*gmr>dNek2-GFP,* Ret^{MEN2B}*, PI3K−/+, S6K−/+*; Figure 5d). Moreover, when we fed *dNek2*-overexpressing flies with drugs that inhibited signaling at different points along the PI3K cascade—LY294002 (PI3K inhibitor), Rapamycin (Tor inhibitor), MK2206 (Akt inhibitor), BEZ235 (dual PI3K/Tor inhibitor)—we significantly suppressed distant seeding of cells (Figure 5d). Finally, cooperation between *Nek2* and *Ras* plus *Src* signaling was also suppressed by inhibition of the PI3K pathway. *dNek2; Csk−/−;* Ras^{V12} *eyeless-FLPase-MARCM* larvae fed with MK2206 showed significantly smaller primary tumors and complete absence of secondary tumors (Figures 5e and f). In summary, our genetic interaction and inhibitor studies showed that the PI3K-Akt pathway was a key mediator of cooperativity between dNek2 and other oncogenic signaling pathways.

In silico identification of Nek2-inhibitory drug-like candidates

Suitable non-toxic small molecule inhibitors of human Nek2 (hNek2) remain commercially unavailable. A rational computational approach was undertaken to first identify drug-like compounds from a small library that could potentially inhibit human Nek2 kinase *in vitro*. In analyzing the primary sequence and crystallographic structures of Nek2, we noticed that there exists a uniquely conserved helical motif (αT) in Nek2 immediately following the DFG motif also present in EGFR and HER2 kinases.[13] As this αT motif has a dynamic role in kinase activation, we surmised that EGFR/HER2 inhibitors that interact with the αT motif might also inhibit the activity of Nek2 kinase. While the sequence alignments of Nek2 (PDB ID: 2JAV)[14] with that of EGFR (PDB ID: 2JIV)[28] and HER2 (PDB ID: 3PP0)[29] revealed only 22% sequence identity (45% sequence similarity) and 27% sequence identity (49% sequence similarity), respectively, the tertiary folds were remarkably similar (Figure 6a and Supplementary Figure S1). A comparative analysis of the crystal structure of an ATP-site directed, Nek2-bound pyrroleindolinone inhibitor and the *in silico* docked pyrroleindolinone complex of EGFR and HER2 further revealed that a significant binding overlap existed between the three complexes (>55% similar inhibitor-active site residue interactions; Figure 6b). Significant similarities of interactions observed in all three inhibitor-bound complexes, along with similarities in secondary structural elements, indicated that certain existing EGFR/HER2 inhibitors might also inhibit Nek2 activity.

Before testing existing EGFR/HER2 inhibitors as potential Nek2 inhibitors *in silico*, we first validated our computational Glide docking algorithm on previously reported Nek2 inhibitors (Supplementary Table S1). After validating our computational strategy, we assembled a set of 27 commercially available preclinical and clinical stage EGFR/HER2 inhibitors and investigated *in silico* for their potential to serve as Nek2 inhibitors. Using a stringent selection criteria based on both the Glide scoring function and the visual inspection (Supplementary Information), a set of seven EGFR/HER2 inhibitors were chosen for *in vitro* evaluation (Supplementary Table S2). Among these, neratinib (Glidescore = −7.93 kcal/mol) was found to be the top scoring compound with desired structural attributes, with pelitinib as the second best (Glidescore = −7.86 kcal/mol). Structural analysis of the molecular interaction of neratinib within the active site of Nek2 revealed a number of important binding features (Figure 6c and Supplementary Information). Interestingly, many of these interactions are also exhibited by pelitinib bound to Nek2-active site (data not shown).

EGFR/HER2 inhibitors inhibit human Nek2 activity *in vitro* reversibly

After identifying seven EGFR/HER2 inhibitors as potential Nek2 inhibitors from our *in silico* screen, we tested their ability to inhibit the recombinant human Nek2 at 10 μM concentration using ^{32}P-ATP-based assay (Supplementary Information). We identified neratinib and pelitinib as our lead Nek2-inhibitory compounds (>28% hit rate; Figure 6d). A comparison of these two compounds revealed that they both contained a bicyclic, 6,7-disubstituted-4-(arylamino)quinoline-3-carbonitrile motif. Slightly reduced activity of pelitinib as compared with neratinib might be due to lack of 4-pyridylmethoxy substituent, which is involved in hydrophobic interactions with the key α-T helix residues, Gly161, Leu162 and Ala163. Interestingly, other known EGFR/HER2 inhibitors such as afatinib, canertinib and gefitinib, containing a bicyclic *N*-(3-chloro-4-fluorophenyl)quinazolin-4-amine moiety, did not display any inhibition even at 20 μM. The poor activity of these three inhibitors against Nek2 may be explained based on the nature of substituent at the 7-position of the quinazoline ring. For example, these structures carry either very small methoxy group or very bulky oxolanyloxy and morpholinylpropoxy substituent at this position instead of the optimal ethoxy group. Similarly, mono and disubstituted *N*-(aryl)quinazolin-4-amine containing EGFR inhibitors, erlotinib and lapatinib, were not inhibitory under these conditions. Bulky methoxypropoxy substituent at 7-position in case of erlotinib and the absence of any group at 7-position in case of lapatinib may be responsible for this dramatic loss of activity. It should be noted here that both neratinib and pelitinib are known covalent and irreversible inhibitors of EGFR and HER2. A dose–response analysis revealed that neratinib and pelitinib displayed a remarkable potency, and inhibited hNek2 with IC-50 values of 247 nM and 661 nM, respectively (Figure 6e). No time-dependent inhibition was observed even on prolonged incubation (30 min) of neratinib and pelitinib with hNek2. This indicated that despite the presence of electrophilic crotonamide functionality, the mode of hNek2 inhibition by these compounds was non-covalent and reversible in nature. This is not surprising as Cys797 of EGFR and the corresponding Cys805 of HER2 to which neratinib establishes covalent bond is replaced by the Asp93 of Nek2 (Figure 6b).

Subset of EGFR/HER2 inhibitors inhibit dNek2 function in whole-animal assays

Next we tested the ability of neratinib and pelitinib to effectively inhibit dNek2 function *in vivo* using our fly overexpression model. When increasing doses of these two drugs were fed to developing larvae, the adult distant seeding phenotype was strongly

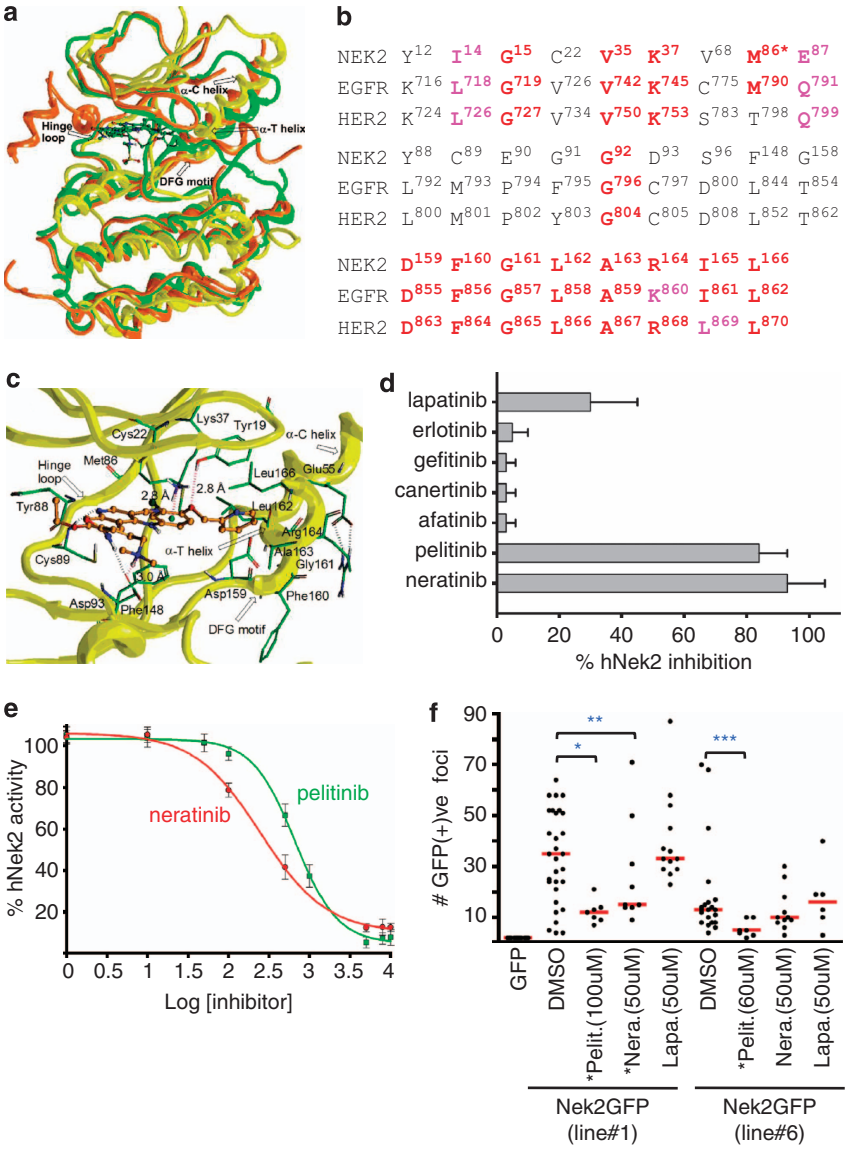

Figure 6. (**a**) Superimposition of Nek2 (PDB ID: 2JAV), EGFR (PDB ID: 2JIV) and HER2 (PDB ID: 3PP0) kinases. Nek2, EGFR and HER2 are shown as yellow, orange and green colored ribbon models, respectively. Key conserved residues are also shown as stick model with color scheme by element type as implemented in Maestro. (**b**) An analysis of the residues present within 5 Å distance from the bound pyrroleindolinone inhibitor in the co-crystal structure of hNek2 (PDB ID: 2JAV), and the corresponding residues at the equivalent positions from the *in silico* docked complex of EGFR and HER2 kinases. A total of 26 residues are compared; red color, identical residues; pink color, similar residues; black color, no homology; *Met86; Thr86 in wild type; Nek2/EGFR: 12 identical, 3 similar, 11 with no homology; Nek2/HER2: 11 identical, 3 similar, 12 with no homology. (**c**) Binding model of neratinib within the active site of human Nek2 kinase (left). Important amino acids are depicted as sticks with the atoms colored as carbon—green, hydrogen—white, nitrogen—blue, oxygen—red, sulfur—yellow. Neratinib is shown as ball and stick model with the same color scheme as above except carbon atoms are represented in orange and chloro atom as green. Anilino ring centroid is displayed as green sphere. Dotted black line indicates hydrogen bonding interaction, whereas dotted red line indicates possible hydrogen bonding and ionic interactions with distances in Å. (**d**) Inhibitory screening profile of selected small molecule library compounds against wild-type (wt) human Nek2 kinase. The screening was performed at 10 μM inhibitory concentrations. (**e**) Dose–response curves for neratinib- (red circle) and pelitinib-mediated (green square) inhibition of wt human Nek2 kinase. The points are experimental and the line joining them is the fit to obtain the IC-50 values for neratinib as 247 nM and pelitinib as 661 nM, respectively. (**f**) Nek2-driven cell migratory phenotype (distant seeding; foci in GFP alone compared with Nek2GFP flies fed with DMSO) is suppressed upon treatment with pelitinib in two transgenic fly lines (#1 and #6) and upon treatment with neratinib in one fly line (#1). Distant seeding quantitation was performed as in Figure 5. Asterisks indicate *P*-values <0.05, in a two-tailed students *t*-test.

suppressed. Quantitation of the number of total GFP + foci with one dNek2-GFP transgenic line showed a decrease in the median number of foci from ~37/animal (untreated) to ~10/animal (pelitinib) and ~15/animal (Neratinib) after inhibitor treatment. Similar suppression of 'distant seeding' was observed with a second dNek2-GFP transgenic line (*gmr>dNek2-GFP*; Figure 6f). Interestingly lapatinib, which had showed modest inhibition of Nek2 *in vitro* had no effect on the distant seeding phenotype (Figure 6f). Thus, our whole-animal model successfully discriminated between compounds that inhibited Nek2 activity *in vitro* with those that actually suppressed Nek2 activity *in vivo*.

Human Nek2 activates Akt and β-catenin pathways and can be inhibited by compounds identified in *Drosophila*

We next investigated whether our findings on *Drosophila* Nek2 function translated to human cells. We overexpressed human Nek2 (hNek2) in A549 lung adenocarcinoma cell lines, which has been shown to express high levels of K-Ras.[30] A549 cells also have low levels of endogenous Nek2 making this an ideal cell type to test the consequences of hNek2 overexpression (Figure 7b). Transient overexpression of hNek2 in A549 cells led to activation of the Akt pathway (increase in pAkt and pS6), phosphorylation of GSK3β, stabilization of β-catenin, as well as activation of pJNK and deregulation of Rac1 levels, all of which had parallels to our *Drosophila* studies (Figures 7a and b). Interestingly, hNek2 overexpression in A549 cells led to a severe reduction of β-catenin signal at the cell–cell adherens junction complexes and increase of β-catenin signal in and around the nucleus (Figure 7a). Reduced β-catenin in the adherens junction and its translocation to the nucleus is indicative of invasive state of cells, thus further supporting our hypothesis that Nek2 regulates invasion/metastasis. hNek2 overexpression in non-cancerous HEK293T cells led to deregulation of pAkt, pS6, pGSK3β, β-catenin, RhoA, pJNK, levels indicating that these pathways are activated by Nek2 even in non-tumorigenic human cells (Figure 7c). Finally, we tested whether inhibiting hNek2 and the Akt pathway with the compounds we identified in flies would suppress signaling initiated by hNek2. Indeed both pelitinib and MK2206 suppressed hNek2-dependent increase in cytosolic β-catenin and pJNK, and also partially restored the deregulation of RhoA and pS6 levels (Figure 7d).

Together these results demonstrate that potent non-toxic Nek2 inhibitors can be identified using our whole-animal fly assay and that these compounds can inhibit Nek2 activity in human cells. Importantly, the fact that pelitinib, although less effective *in vitro* in inhibiting hNek2 kinase activity, was more effective in inhibiting the distant seeding phenomenon *in vivo* further reinforces the need to include *in vivo* models in early drug discovery efforts. On the basis of our studies, we propose that a novel Nek2-targeting anti-cancer agent with low cellular toxicity can be developed based on the bicyclic, 6,7-disubstituted-4-(arylamino)quinoline-3-carbonitrile motif we have identified in our studies (Figure 8b).

DISCUSSION

Current thinking is that Nek2, like other centrosomal kinases, could promote cancer progression by enhancing various mitotic abnormalities that lead to CIN.[31] Nek2 has not been implicated in early stages of cancer progression, for example, by promoting proliferation, survival and invasion. It is postulated that CIN is a late stage characteristic of cancer, providing initiating driver

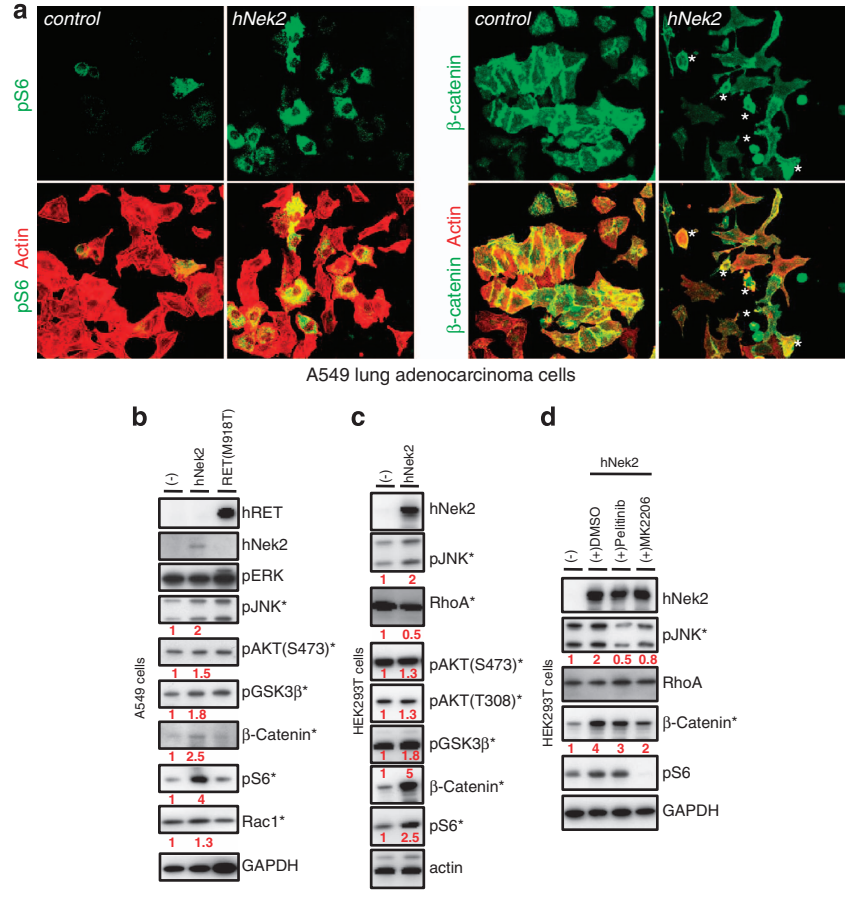

Figure 7. (**a**) Transient transfection of hNek2 in A549 cells led to upregulation of Akt pathway marker pS6, and strong deregulation of β-catenin levels. In mock-transfected cells β-catenin is at the cell–cell junctions but hNek2-transfected cells show strong reduction of β-catenin from the junctions. Note that some Nek2-transfected cells (asterisk) show increased β-catenin in and around the nucleus. (**b**) Western analysis of transiently transfected hNek2 in A549 cells shows upregulation of pAkt, pS6, pGSK3β, β-catenin, pJNK and Rac1 levels. Deregulated proteins indicated with asterisk. Constitutively active RET, hRETM918T, which is known to activate these pathways (pErk, pJNK, pAkt) is used as control. [40] (**c**) Western analysis of transiently transfected hNek2 in HEK293T cells shows upregulation of pAkt, pS6, pGSK3β, β-catenin, pJNK and downregulation of RhoA. Relative levels of proteins between control and hNek2 overexpressing cells are indicated in red. (**d**) Nek2-dependent upregulation of β-catenin and pJNK, in HEK293T cells can be inhibited by addition of pelitinib or Akt inhibitor MK2206. Inhibitors were added at a concentration of 0.5 μM for 2 h, following 24 h of growth and transfection of cells.

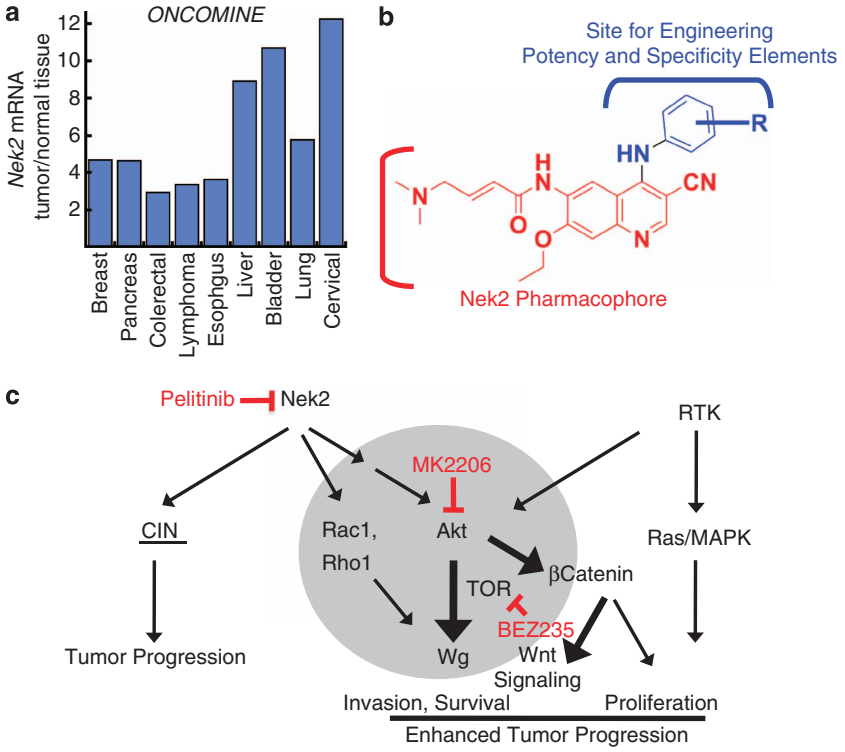

Figure 8. (**a**) Analysis of Oncomine data showed that median *hNek2* mRNA levels were consistently upregulated in patient tumors in the following cancers—breast,[41] pancreas,[42] colorectal,[43] lymphoma,[44] esophagus,[45] liver,[46] bladder,[47] lung,[48] and cervical.[49] (**b**) The chemical structure of Nek2 pharmacophore identified for possible SAR studies. (**c**) Model showing how Nek2 signaling can promote metastasis by cooperating with mitogen-activated protein kinase (MAPK) and RTK signaling; chromosomal instability (CIN). The PI3K-Akt pathway is an axis through which Nek2 cooperates with other pathways, indicated by heavy black arrow. Akt pathway upregulation would inhibit GSK3β leading to stabilization of β-catenin and increase in Wnt signaling. Wingless/Wnt itself is also upregulated by Nek2 expression, creating the possibility of a complex feedback loop through interaction with other signaling pathways such as the Hippo cascade.[50] Red inhibitory signs indicate points along the signaling cascade where we can pharmacologically inhibit Nek2-driven tumorigenesis more effectively.

mutations with source of genetic variation through which to promote tumorigenesis.

We show, for the first time, that Nek2 overexpression in combination with oncogenic signaling pathways can promote invasion and metastasis through combinatorial activation of the Akt pathway, stabilization of β-catenin, upregulation of Wnt/Wg, inhibition of apoptosis and deregulation of the Rho1-Rac1 balance. As activation of the Akt, β-catenin and Wnt pathways can promote growth, survival as well invasion, acquisition of increased Nek2 activity in tumors could also promote early stage cancer progression. Invasion is the first step toward eventual metastasis, the cause of most cancer-related deaths. During the process of submission of our manuscript, one study showed that human Nek2 can activate the Akt pathway to promote drug resistance in myeloma, once again supporting our conclusions.[32] Our findings implicate Nek2 in a novel and important role in the process of tumor progression, that is, metastasis (Figure 8c; model), indicating why Nek2 is frequently overexpressed in many cancers.

Overactive RTK as well as Ras and Src signaling is common to a number of cancer types, for example in the lung (EGFR), breast (HER2), thyroid (RET), pancreas (EGFR).[33] Therefore, the potential for Nek2 to synergize with other oncogenic signaling pathways, like we have shown in *Drosophila*, and drive progression of a wide range of cancers is enormous. Our own survey of the Oncomine data set shows that *Nek2* mRNA is indeed overexpressed in a number of cancer types (Figure 8a). In the future, it would be useful to analyze these data sets to ascertain if Nek2 levels progressively increase as tumors become more invasive and metastatic. Our studies show that indeed hNek2 overexpression in human lung cancer cells can activate the same pathways that we identified in our fly studies.

Our findings on Nek2 have a remarkable parallel to that of another centrosomal kinase Aurora-A. Recent evidence suggests that Aurora-A overexpression also induces Akt activation.[34] Taken together, these findings strongly suggest that centrosomal kinases, for example, *Nek2* and *Aurora-A*, can also activate the Akt pathway and promote survival and/or invasion/migration and metastasis during cancer progression. This posits a novel role for centrosomal kinases beyond the conventional CIN. The notion that deregulation of proteins that control the integrity of proper nuclear division promote tumorigenesis only through CIN has recently been challenged. Loss of spindle assembly checkpoint components resulted in basal delamination of epithelial cells and invasion in *Drosophila*,[35] thus further supporting our findings that cellular components previously thought to promote cancer through CIN could also promote invasion and metastasis. It might also provide an explanation as to why centrosomes are frequently amplified in many cancers.

Our studies also make important predictions about how to strategically inhibit cancers with Nek2 overexpression (Figure 8c). We suppressed the ability of dNek2 to cooperate with other oncogenic signaling axes through inhibition of the PI3K pathway. PI3K pathway inhibitors, either singly or in combination, could be an effective treatment for patients with high levels of Nek2. Another key finding from our studies is that certain EGFR/HER2 inhibitors can inhibit Nek2 activity. This postulates a provocative notion that clinical success of some of the EGFR/HER2 inhibitors could actually arise from inhibition of both EGFR/HER2 as well as Nek2. This is a testable hypothesis.

Cancer cell lines where EGFR and Nek2 are both overactive should respond better to dual Nek2/EGFR inhibitors such as pelitinib and neratinib, compared with EGFR-specific inhibitors such as gefitinib and erlotinib. Our studies also reveal that novel drug-like Nek2-inhibitory pharmacophore with *in vivo* activity can be identified using our developed Nek2 fly model. Our work lays the framework for future studies that can further dissect the role of Nek2 in cancer progression as well as develop more effective strategies to inhibit the cancer-promoting Nek2 pathway.

MATERIALS AND METHODS

Generation of dNek2-GFP model, fly stocks and genetics

The gene encoding the *D. melanogaster* Nek2 kinase was PCR amplified from a cDNA and was inserted into the *Not*I and *Xho*I restriction sites of the pUAST vector containing a C-terminal GFP tag to obtain *in vivo* fluorescent Nek2 proteins for intracellular imaging experiments. The identity of clones was verified by dideoxy sequencing. *dNek2-GFP-pUAST* DNA was microinjected into *Drosophila* embryos using standard techniques (BestGene Inc., Chino Hills, CA, USA). The following fly stocks were used: *UAS-Ret*^{MEN2B},[10] and *FRT 82B Csk*^{null} $-/+$; *UAS Ras*^{V12}. For the eyeless-FLP MARCM experiments, *y,w,eyFLP1; Act5C>y*$^{+}$*>Gal4, UAS-GFP; P[FRT]82B tub-Gal80* female virgins were crossed to *P[FRT]82B UASdRet*^{MEN2B} or *P[FRT]82B UASdRet*^{MEN2B}; *UASdNek2-GFP*, or *P[FRT]82B Csk*^{null} $-/+$; *UASRasV12*, and *UASdNek2-GFP; P[FRT]82B Csk*^{null} $-/+$, *UASRasV12* males and their progeny were raised in regular food. All flies were raised at 25 °C using standard fly genetics.

Histology and antibodies

Third instar wing discs were staged and fixed in 4% paraformaldehyde. Immunofluorescence was performed as described.[36] Antibodies used were: β-catenin, Rac1 (BD Biosciences, San Jose, CA, USA); pRet, pJnk, pAkt, pS6, pGSK3β (Cell Signaling, Danvers, MA, USA); pSrc(Y^{418}) (Invitrogen, Grand Island, NY, USA); pERK, GFP (Sigma, St Louis, MO, USA); Arm, Ecad, Rho1, α-tubulin, Syntaxin, Mmp1, Wg, CycE (Developmental Studies Hybridoma Bank, Iowa City, IA, USA); gamma-tubulin, RhoA (Santa Cruz Biotechnology, Santa Cruz, CA, USA); and anti-DIAP1 (from H. Steller).

Quantitation of GFP foci in dNek2-GFP flies and live imaging of adult eyes

dNek2-GFP flies (lines #1 and #6) were crossed to *GMR-Gal4* flies and placed in vials containing different concentrations of the drugs, lapatinib, pelatinib and neratinib, LY294002, Rapamycin, BEZ235, MK2206 or DMSO (control). F1 progeny from the above crosses were scored for GFP-positive eye phenotype and photographed using Leica M165FC fluorescence stereoscope (Leica, Buffalo Grove, IL, USA). GFP-positive flies were further analyzed for GFP foci in distant locations in the body, such as the wings, legs, head and whole body. The GFP foci were quantitated and compared in the drug-treated versus untreated control flies. The results were graphed and subjected to statistical analysis using the PRISM-Graphpad Software. Progeny of the eyeless-FLP MARCM experiments were imaged in a similar manner with combined bright-light and fluorescence settings.

Tissue culture studies

The gene encoding WT human Nek2 was PCR amplified from a pGEM plasmid containing the Nek2 gene and cloned into pCMV vector. A549 and HEK293T cells were grown in RPMI1640 and DMEM media, respectively, supplemented with 10% FBS and penicillin-streptomycin mix. Cells were transfected with lipofectamine and cell lysis performed 24 and 48 h after transfection. For imaging studies, cells were grown to 50% confluency in Lab-TekII 8-chamber slides (Fisher, Pittsburgh, PA, USA), transfected and grown for further 24 h in serum-free media.

Tumor cell injection into adult flies

Third instar larval eyeless-FLP MARCM eye discs (GFP^{+}) of the indicated genotype were dissected in 1 × PBS on ice and dissociated in a solution of artificial hemolymph[37] (10 eye discs per fixed volume) in a 1.7-ml eppendorf tube using a small plastic pestle. Dissociated tissue solution was loaded onto a fine tipped needle and approximately equal volumes were injected into the dorsal region of the notum of an adult fly using a microinjector. Flies were allowed to recover and placed in fly food vials and monitored for GFP expression every couple of days. The tumor cell injection assay is an adaptation from a cell injection assay developed by Tzou *et al*.[38]

Western blot analysis

Ten third instar discs of each genotype were dissolved in lysis buffer (50 mM Tris, 150 mM NaCl, 1% TritonX-100, 1 mM EDTA) supplemented with protease inhibitor cocktail (Sigma) and phosphatase inhibitor cocktail (Sigma). Total protein in each sample was quantitated using Bio-Rad protein assay (Bio-Rad Laboratories, Hercules, CA, USA). Samples were boiled, resolved on SDS–PAGE and transferred by standard protocols. Membranes were stripped with Sigma Restore stripping buffer and reprobed with other antibodies to assess signal under exactly the same loading conditions.

Computational analysis

For obtaining a three-dimentional structure of *Drosophila* Nek2 kinase, homology modeling was performed using the Prime software (Schrödinger Inc., New York, NY, USA) with human Nek2 (PDB: 2JAV) as a template. For docking studies, the initial protein structure of Nek2 along with crystallographic water molecules was refined by means of default parameters mentioned in protein preparation tool implemented in Maestro v9.0 and Impact program v5.5. The protonation states of residues were adjusted to the dominant ionic forms at pH 7.4. Refined protein was further used to generate a grid by selecting bound inhibitor pyrroleindolinone. The grid thus generated was further used for docking of a focused library of EGFR/HER2 kinase inhibitors at the active site of Nek2. Commercially available small molecule drug library comprising of 27 clinically investigated EGFR/HER2 inhibitors (Selleck Chemicals, Houston, TX, USA and LC Laboratory, Woburn, MA, USA) were built using the fragment dictionary of Maestro v9.0 and energy minimized by Macromodel program v9.7 (Schrödinger Inc.) using the OPLSAA force field with the steepest descent followed by truncated Newton conjugate gradient protocol. The low-energy 3D structures of all compounds were generated by LigPrep v2.3: different protonation states at physiological pH ± 2, all possible tautomers and ring conformations. In a similar manner, 10 known Nek2 inhibitors were also processed for the validation of our docking strategy. The output of Ligprep run comprising of a total of 37 compounds was used as input for docking experiments. Docking of a set of 27 EGFR/HER2 inhibitors and 10 known Nek2 inhibitors within the active site of Nek2 was performed using the 'Extra Precision' (XP) mode of Glide docking program v5.5 and the default parameters. All computations were carried out on a Dell Precision 47n dual processor with the Linux OS (Red Hat Enterprise WS, Raleigh, NC, USA).

Acquisition of recombinant human Nek2 kinase, *in vitro* screening and IC-50 determination

The gene encoding WT Nek2 was PCR amplified from a pGEM plasmid containing the *Nek2* gene. C-terminally $(His)_6$-tagged Nek2 enzyme was achieved by incorporating the *Nek2* gene into pET32a. The WT lambda protein phosphatase (LPP2) open reading frame was PCR amplified from the lambda genomic DNA and inserted into the pET22b expression vector. Nek2 and LPP2 –pET22b vectors were co-transformed into BL21 (RIPL) codon plus *E. coli* cells and expressed under isopropyl-β-D-thiogalactoside induction, as described earlier.[14] Overexpressed proteins were purified to homogeneity by a metal-affinity Ni-NTA column followed by SP-sepharose column and evaluated for appropriate activity (Supplementary Figures S2 and S3). All *in vitro* Nek2 kinase assays were performed in triplicates at 25 °C at pH 7.5 in a kinase assay buffer (50 mM Tris HCl, 2 mM dithiothreitol, 0.3 mg/ml bovine serum albumin, 0.5 mM Na_2EDTA) using wild-type human Nek2 enzyme. For *in vitro* enzyme assay, a peptide-based Nek2 substrate, Ac-IRRLSTRRR-$CONH_2$,[39] was synthesized by standard Fmoc-chemistry and used (Supplementary Information). See Supplementary Information for determination of IC-50 values.

CONFLICT OF INTEREST

The authors declare no conflict of interest.

ACKNOWLEDGEMENTS

We thank Professor Andrew M Fry, University of Leicester, UK for sharing human Nek2 kinase plasmid, and Biology Department, Queens College for allowing the use

of the core facility. We also thank Marek Mlodzik, Ursula Weber, Carlo Iomini, Ivan Plaza-Menacho for sharing antibodies, fly stocks and DNA constructs. This work was supported by NIH/NCI grants R01-CA084309 and R01-CA109730 to RLC, American Cancer Society Grant 120886-PFM-11-137-01-DDC to TKD, NIGMS training grant T32 GM-62754, NIH to JP, and Professional Staff Congress—CUNY grant 64492-00 42 to SK.

AUTHOR CONTRIBUTIONS

TKD and SK conceived the fly Nek2 model. TKD conceived the tumor cell injection assay, performed *in vivo* fly assays, fly genetics, westerns, immunofluorescence studies and imaging experiments. TKD generated pCMV-hNek2 vector, designed and performed vertebrate tissue culture studies. SKP generated dNek2-UAS construct and generated recombinant hNek2 protein. SK and TKD conceived the inhibitor screen. SK funded the development of fly model and inhibitor screen. DD, HJ and SK performed *in vitro* experiments to assess inhibitory potential of library compounds. SSP performed evaluation of distant seeding phenotype to assess the *in vivo* efficacy of drugs/inhibitors and some fly imaging experiments. SS and TTT performed molecular modeling studies. JP performed tumor cell injection assays. RLC supported the fly studies. All authors read and commented on the manuscript. SK and TKD guided the overall project and wrote the manuscript.

REFERENCES

1 Schvartzman JM, Sotillo R, Benezra R. Mitotic chromosomal instability and cancer: mouse modelling of the human disease. *Nat Rev Cancer* 2010; **10**: 102–115.
2 Li JJ, Li SA. Mitotic kinases: the key to duplication, segregation, and cytokinesis errors, chromosomal instability, and oncogenesis. *Pharmacol Ther* 2006; **111**: 974–984.
3 Fry AM. The Nek2 protein kinase: a novel regulator of centrosome structure. *Oncogene* 2002; **21**: 6184–6194.
4 Rajagopalan H, Lengauer C. Aneuploidy and cancer. *Nature* 2004; **432**: 338–341.
5 Hayward DG, Clarke RB, Faragher AJ, Pillai MR, Hagan IM, Fry AM. The centrosomal kinase Nek2 displays elevated levels of protein expression in human breast cancer. *Cancer Res* 2004; **64**: 7370–7376.
6 Kokuryo T, Senga T, Yokoyama Y, Nagino M, Nimura Y, Hamaguchi M. Nek2 as an effective target for inhibition of tumorigenic growth and peritoneal dissemination of cholangiocarcinoma. *Cancer Res* 2007; **67**: 9637–9642.
7 Sharma SV, Haber DA, Settleman J. Cell line-based platforms to evaluate the therapeutic efficacy of candidate anticancer agents. *Nat Rev Cancer* 2010; **10**: 241–253.
8 Cheon DJ, Orsulic S. Mouse models of cancer. *Annu Rev Pathol* 2011; **6**: 95–119.
9 Herranz H, Hong X, Hung NT, Voorhoeve PM, Cohen SM. Oncogenic cooperation between SOCS family proteins and EGFR identified using a *Drosophila* epithelial transformation model. *Genes Develop* 2012; **26**: 1602–1611.
10 Das TK, Sangodkar J, Negre N, Narla G, Cagan RL. Sin3a acts through a multi-gene module to regulate invasion in *Drosophila* and human tumors. *Oncogene* 2012; **32**: 3184–3197.
11 Rudrapatna VA, Cagan RL, Das TK. *Drosophila* cancer models. *Dev Dynam* 2012; **241**: 107–118.
12 Gonzalez C. *Drosophila melanogaster:* a model and a tool to investigate malignancy and identify new therapeutics. *Nat Rev Cancer* 2013; **13**: 172–183.
13 Dar AC, Das TK, Shokat KM, Cagan RL. Chemical genetic discovery of targets and anti-targets for cancer polypharmacology. *Nature* 2012; **486**: 80–84.
14 Rellos P, Ivins FJ, Baxter JE, Pike A, Nott TJ, Parkinson DM *et al.* Structure and regulation of the human Nek2 centrosomal kinase. *J Biol Chem* 2007; **282**: 6833–6842.
15 Westwood I, Cheary DM, Baxter JE, Richards MW, van Montfort RL, Fry AM *et al.* Insights into the conformational variability and regulation of human Nek2 kinase. *J Mol Biol* 2009; **386**: 476–485.
16 Brand AH, Perrimon N. Targeted gene expression as a means of altering cell fates and generating dominant phenotypes. *Development* 1993; **118**: 401–415.
17 Huang H, Du G, Chen H, Liang X, Li C, Zhu N *et al. Drosophila* Smt3 negatively regulates JNK signaling through sequestering Hipk in the nucleus. *Development* 2011; **138**: 2477–2485.
18 Swarup S, Verheyen EM. Wnt/Wingless signaling in *Drosophila*. *Cold Spring Harb Perspect Biol* 2012; **4**: 6.
19 Hanahan D, Weinberg RA. Hallmarks of cancer: the next generation. *Cell* 2011; **144**: 646–674.
20 Dillon RL, Muller WJ. Distinct biological roles for the akt family in mammary tumor progression. *Cancer Res* 2010; **70**: 4260–4264.
21 Parri M, Chiarugi P. Rac and Rho GTPases in cancer cell motility control. *Cell Commun Signal* 2010; **8**: 23.
22 Read RD, Goodfellow PJ, Mardis ER, Novak N, Armstrong JR, Cagan RLA. *Drosophila* model of multiple endocrine neoplasia type 2. *Genetics* 2005; **171**: 1057–1081.
23 Pagliarini RA, Xu T. A genetic screen in *Drosophila* for metastatic behavior. *Science* 2003; **302**: 1227–1231.
24 Vidal M, Warner S, Read R, Cagan RL. Differing Src signaling levels have distinct outcomes in *Drosophila*. *Cancer Res* 2007; **67**: 10278–10285.
25 Janic A, Mendizabal L, Llamazares S, Rossell D, Gonzalez C. Ectopic expression of germline genes drives malignant brain tumor growth in *Drosophila*. *Science* 2010; **330**: 1824–1827.
26 Valenta T, Hausmann G, Basler K. The many faces and functions of beta-catenin. *EMBO J* 2012; **31**: 2714–2736.
27 Witte HT, Jeibmann A, Klambt C, Paulus W. Modeling glioma growth and invasion in *Drosophila melanogaster*. *Neoplasia* 2009; **11**: 882–888.
28 Yun CH, Mengwasser KE, Toms AV, Woo MS, Greulich H, Wong KK *et al.* The T790M mutation in EGFR kinase causes drug resistance by increasing the affinity for ATP. *Proc Natl Acad Sci USA* 2008; **105**: 2070–2075.
29 Aertgeerts K, Skene R, Yano J, Sang BC, Zou H, Snell G *et al.* Structural analysis of the mechanism of inhibition and allosteric activation of the kinase domain of HER2 protein. *J Biol Chem* 2011; **286**: 18756–18765.
30 Telang S, Nelson KK, Siow DL, Yalcin A, Thornburg JM, Imbert-Fernandez Y *et al.* Cytochrome c oxidase is activated by the oncoprotein Ras and is required for A549 lung adenocarcinoma growth. *Mol Cancer* 2012; **11**: 60.
31 Hayward DG, Fry AM. Nek2 kinase in chromosome instability and cancer. *Cancer Lett* 2006; **237**: 155–166.
32 Zhou W, Yang Y, Xia J, Wang H, Salama ME, Xiong W *et al.* NEK2 induces drug resistance mainly through activation of efflux drug pumps and is associated with poor prognosis in myeloma and other cancers. *Cancer Cell* 2013; **23**: 48–62.
33 Gschwind A, Fischer OM, Ullrich A. The discovery of receptor tyrosine kinases: targets for cancer therapy. *Nat Rev Cancer* 2004; **4**: 361–370.
34 Wang X, Zhou YX, Qiao W, Tominaga Y, Ouchi M, Ouchi T *et al.* Overexpression of aurora kinase A in mouse mammary epithelium induces genetic instability preceding mammary tumor formation. *Oncogene* 2006; **25**: 7148–7158.
35 Dekanty A, Barrio L, Muzzopappa M, Auer H, Milan M. Aneuploidy-induced delaminating cells drive tumorigenesis in *Drosophila epithelia*. *Proc Natl Acad Sci USA* 2012; **109**: 20549–20554.
36 Brachmann CB, Jassim OW, Wachsmuth BD, Cagan RL. The *Drosophila* bcl-2 family member dBorg-1 functions in the apoptotic response to UV-irradiation. *Curr Biol* 2000; **10**: 547–550.
37 Singleton K, Woodruff RI. The osmolarity of adult *Drosophila* hemolymph and its effect on oocyte-nurse cell electrical polarity. *Dev Biol* 1994; **161**: 154–167.
38 Tzou P, Meister M, Lemaitre B. Methods for studying infection and immunity in Drosophila. In: *Methods in Microbiology,* Vol. 31. Elsevier, 2002, pp 507–529, http://dx.doi.org/10.1016/S0580-9517(02)31028-6.
39 Fry AM, Schultz SJ, Bartek J, Nigg EA. Substrate specificity and cell cycle regulation of the Nek2 protein kinase, a potential human homolog of the mitotic regulator NIMA of *Aspergillus nidulans*. *J Biol Chem* 1995; **270**: 12899–12905.
40 Plaza-Menacho I, Morandi A, Mologni L, Boender P, Gambacorti-Passerini C, Magee AI *et al.* Focal adhesion kinase (FAK) binds RET kinase via its FERM domain, priming a direct and reciprocal RET-FAK transactivation mechanism. *J Biol Chem* 2011; **286**: 17292–17302.
41 Richardson AL, Wang ZC, De Nicolo A, Lu X, Brown M, Miron A *et al.* X chromosomal abnormalities in basal-like human breast cancer. *Cancer Cell* 2006; **9**: 121–132.
42 Pei H, Li L, Fridley BL, Jenkins GD, Kalari KR, Lingle W *et al.* FKBP51 affects cancer cell response to chemotherapy by negatively regulating Akt. *Cancer Cell* 2009; **16**: 259–266.
43 Hong Y, Downey T, Eu KW, Koh PK, Cheah PYA. 'metastasis-prone' signature for early-stage mismatch-repair proficient sporadic colorectal cancer patients and its implications for possible therapeutics. *Clin Exp Metastasis* 2010; **27**: 83–90.
44 Piccaluga PP, Agostinelli C, Califano A, Rossi M, Basso K, Zupo S *et al.* Gene expression analysis of peripheral T cell lymphoma, unspecified, reveals distinct profiles and new potential therapeutic targets. *J Clin Invest* 2007; **117**: 823–834.
45 Hu N, Clifford RJ, Yang HH, Wang C, Goldstein AM, Ding T *et al.* Genome wide analysis of DNA copy number neutral loss of heterozygosity (CNNLOH) and its relation to gene expression in esophageal squamous cell carcinoma. *BMC Genom* 2010; **11**: 576.
46 Wurmbach E, Chen YB, Khitrov G, Zhang W, Roayaie S, Schwartz M *et al.* Genome-wide molecular profiles of HCV-induced dysplasia and hepatocellular carcinoma. *Hepatology* 2007; **45**: 938–947.
47 Sanchez-Carbayo M, Socci ND, Lozano J, Saint F, Cordon-Cardo C. Defining molecular profiles of poor outcome in patients with invasive bladder cancer using oligonucleotide microarrays. *J Clin Oncol* 2006; **24**: 778–789.

48 Hou J, Aerts J, den Hamer B, van Ijcken W, den Bakker M, Riegman P *et al.* Gene expression-based classification of non-small cell lung carcinomas and survival prediction. *PLoS One* 2010; **5**: e10312.
49 Scotto L, Narayan G, Nandula SV, Arias-Pulido H, Subramaniyam S, Schneider A *et al.* Identification of copy number gain and overexpressed genes on chromosome arm 20q by an integrative genomic approach in cervical cancer: potential role in progression. *Genes Chromosomes Cancer* 2008; **47**: 755–765.
50 Ohsawa S, Sato Y, Enomoto M, Nakamura M, Betsumiya A, Igaki T. Mitochondrial defect drives non-autonomous tumour progression through Hippo signalling in *Drosophila*. *Nature* 2012; **490**: 547–551.

Supplementary Information accompanies this paper on the Oncogenesis website (http://www.nature.com/oncsis).